Ultrafast Dephasing of Surface Plasmon Excitation in Silver Nanoparticles: Influence of Particle Size, Shape, and Chemical Surrounding

J. Bosbach,* C. Hendrich, F. Stietz, T. Vartanyan,† and F. Träger

Fachbereich Physik, and Center for Interdisciplinary Nanostructure Science and Technology–CINSaT, Universität Kassel, Heinrich-Plett-Strasse 40, D-34132 Kassel, Germany

(Received 21 August 2002; published 3 December 2002)

By combination of two special methods, i.e., persistent spectral hole burning and laser assisted nanoparticle preparation, the dephasing time T_2 of surface plasmon excitation in silver nanoparticles was systematically investigated. A strong dependence of T_2 on the plasmon energy is found which reflects the relevance of interband damping and makes necessary a precise control of the particle shape when measuring T_2. The influence of the reduced dimension on the dephasing dynamics was observed as a decrease of T_2 with shrinking particle size. In addition, for silver nanoparticles on quartz substrates, a considerable amount of chemical interface damping was observed.

DOI: 10.1103/PhysRevLett.89.257404 PACS numbers: 78.67.Bf, 61.46.+w, 71.45.Gm, 73.22.Lp

The optical properties of noble- and alkali-metal nanoparticles (NPs) are dominated by collective oscillations of the conduction electrons called *surface plasmons* (SPs) [1]. In contrast to plasmons in bulk matter, these oscillations can be excited with light and lead to distinct resonances in the optical spectra. Recently, the ultrafast dephasing of the SP, that occurs on a time scale of only few femtoseconds, has gained a lot of attraction [2–7]. Reasons are that the dephasing time T_2, being connected to the homogeneous linewidth Γ_{hom} of the resonances via $T_2 = 2\hbar/\Gamma_{\mathrm{hom}}$, is highly interesting by itself and, furthermore, is directly proportional to the local field enhancement, an effect which increases the intensity of the incident light near the NPs surface by several orders of magnitude [1]. Since many devices involving NPs benefit from this effect, T_2 is considered a key parameter for applications such as surface enhanced Raman scattering [8], surface enhanced fluorescence [9], optical tweezers [10], or all-optical switching devices [11]. Furthermore, ultrafast dephasing in the fs regime is still an open question. In order to clarify the role of possible damping processes such as Landau damping, surface scattering of electrons, emission of electrons, and chemical interface damping, systematic investigations are urgently needed. For such studies, however, the size and shape distribution, that ensembles of nanoparticles with sizes of several nanometers usually exhibit, is a major obstacle. These distributions give rise to inhomogeneous line broadening and hamper measurements in the frequency as well as in the time domain [6,12]. A variety of methods have tried to overcome inhomogeneous line broadening, e.g., by spectroscopy of single NPs [4,5,7,13] or generation of NPs with negligible size and shape distributions [6]. Nevertheless, measurements for NPs with dimensions below 15 nm in which the influence of the size, shape and chemical surrounding on T_2 are examined independently, are still lacking.

Recently, measurement of T_2 in silver NPs via a novel technique based on persistent spectral hole burning, has been demonstrated [2,3]. With this method, the influence of inhomogeneous line broadening can be excluded. Advantages of the technique are that it is not restricted to certain particle sizes, does not require special size and shape distributions, and is compatible with ultrahigh vacuum (UHV) conditions, thus allowing for a precise control of the chemical environment. In the present paper, spectral hole burning has been used to systematically determine T_2 of the SP in silver clusters as a function of NP size, shape, and chemical surrounding. Most importantly, we have observed the influence of the reduced dimension of the nanoparticle on the dephasing time T_2.

All experiments were carried out under UHV conditions. Silver NPs were prepared by deposition of silver atoms on sapphire and quartz (0001) surfaces followed by surface diffusion and nucleation. The particle morphology was determined here by combining optical spectroscopy and UHV noncontact atomic force microscopy (AFM) [14]. In short, the results of the characterization are as follows: The generated silver NPs are oblate and their shape can be approximated by rotational ellipsoids. They are characterized by their axial ratio a/b, a and b being the short and long axis, respectively, and their equivalent radius r, i.e., the radius of a sphere with the same volume. For such particles, the SP excitation splits into two modes, their resonance positions depending on the axial ratio. The shape of the NPs depends on their size, i.e., the axial ratio drops off as the radius increases [14]. In view of the size distribution mentioned above, this leads to clusters of different shapes and, consequently, to inhomogeneous broadening of the SP resonances.

Examples of spectral hole burning in the SP (1,1) mode are shown in Fig. 1(a). It depicts extinction spectra of silver NPs with a mean radius of 7 nm at a number density of $1.4 \cdot 10^{11}\,\mathrm{cm}^{-2}$ on a sapphire substrate before and after irradiation with ns–laser pulses of the given fluences. The spectra were recorded at an angle of incidence of 45° using *s*-polarized light of a Xe-arc lamp in

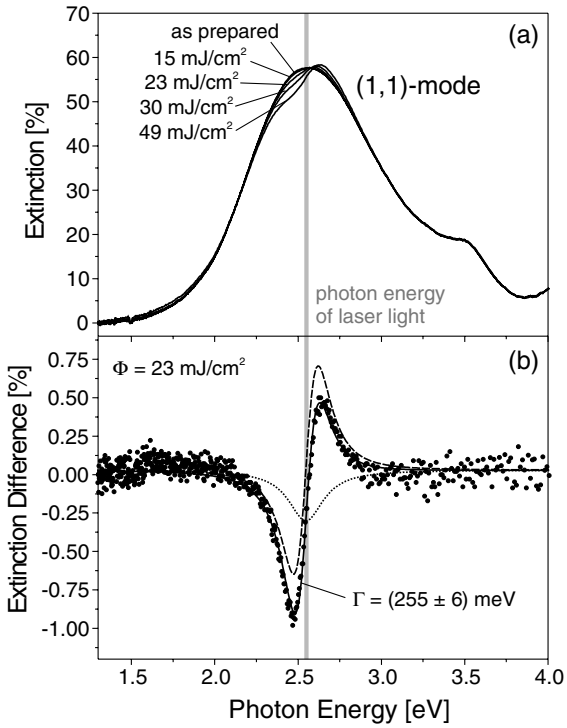

FIG. 1. Spectral hole burning in silver NPs on a sapphire substrate with a photon energy of 2.53 eV (a) Extinction spectra before and after laser irradiation. (b) Difference spectrum for a fluence of $\Phi = 23\,\mathrm{mJ/cm^2}$ (•). For details, see text.

combination with a monochromator. Clearly, the (1,1) SP mode at an energy of 2.6 eV can be detected. For laser irradiation the light of a BBO-OPO (beta-barium borate optical parametrical oscillator) pumped by the third harmonic of a Nd:YAG laser was used. The duration of the OPO pulses was specified to amount from 2 to 4 ns. The laser light was also *s* polarized and the angle of incidence was set to 45°. In subsequent steps 300 laser pulses of fluences between 15 and $49\,\mathrm{mJ/cm^2}$ and a photon energy of 2.53 eV were applied to the NPs, the optical spectrum being recorded after each step. With increasing laser intensity, a spectral hole of growing depth is burned into the optical spectrum. This is revealed in greater detail in the difference spectra between subsequent steps. As an example, Fig. 1(b) shows the difference spectrum for a laser fluence of $23\,\mathrm{mJ/cm^2}$ (•). As can be seen clearly, the spectral hole has an asymmetrical shape. The interaction between the laser light and NPs as well as the resulting change to the optical spectrum has been modeled theoretically and described in detail in Ref. [3]. The resulting changes to the optical spectrum are composed of an even contribution [Fig. 1(b) (dotted line)], describing the shrinkage of the NPs due to thermal desorption of atoms, and an odd contribution [Fig. 1(b) (dashed line)], taking into account the change of the axial ratio due to self-diffusion of atoms. The resulting model function $\delta S(\omega)$ is given by

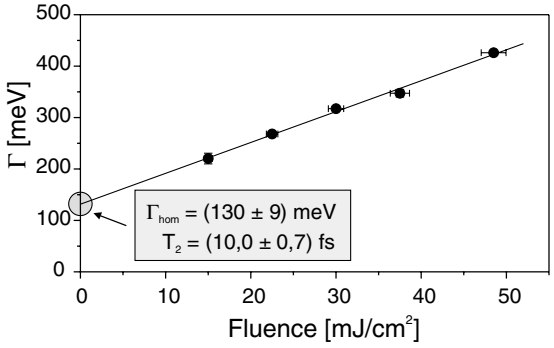

FIG. 2. Width of the spectral holes as a function of laser fluence (•). Linear extrapolation to vanishing fluence (solid line) gives Γ_{hom} for the experiment shown in Fig. 1.

$$\delta S(\omega) = -A\,\frac{(\frac{\Gamma}{2\hbar})^2}{(\omega-\Omega)^2+(\frac{\Gamma}{2\hbar})^2} + B\,\frac{(\omega-\Omega)\,(\frac{\Gamma}{2\hbar})^3}{[(\omega-\Omega)^2+(\frac{\Gamma}{2\hbar})^2]^2}, \qquad (1)$$

where the parameters A and B relatively weight the even and odd contribution, respectively. Ω determines the center of the spectral hole, which is coincident with the laser frequency for small fluences [3], whereas Γ stands for its width. As Fig. 1(b) (solid line) shows, the model function almost perfectly fits the experimental data. For the determination of Γ_{hom}, the fluence dependence of Γ is exploited: The theoretical model predicts a linear convergence towards the homogeneous linewidth for small laser fluences. Figure 2 depicts the values resulting from the data of Fig. 1. Linear extrapolation to zero fluence results in a value of $\Gamma_{\mathrm{hom}} = (130 \pm 9)\,\mathrm{meV}$ for the homogeneous linewidth and of $T_2 = (10.0 \pm 0.7)\,\mathrm{fs}$ for the dephasing time.

As the first step, T_2 was measured as a function of SP energy by tuning the OPO to different wavelengths, Fig. 3 (•). Since the investigated NPs had radii between 9 and 18 nm, they are too large compared to the mean free path of the electrons to observe the influence of the reduced particle dimension as will be shown in the next part of this Letter. On the other hand, the NPs are too small compared to the wavelength of the light to expect appreciable radiation damping [15]. Consequently, the data of Fig. 3 reflects the influence of the bulk dielectric properties of the NPs on the damping process. In terms of classical electrodynamics, Γ_{hom} is expressed through the dielectric function ε with real and imaginary parts ε_1 and ε_2, respectively, by [1,3]

$$\Gamma_{\mathrm{hom}}(\Omega) = \frac{2\,\hbar\,\varepsilon_2(\Omega)}{|\frac{d\varepsilon_1}{d\omega}|_{\omega=\Omega}|}\,. \qquad (2)$$

Using the dielectric function of silver from Ref. [16] and Eq. (2), the experimental data of Fig. 3 is nicely reproduced, Fig. 3 (dashed line). Most remarkable is the strong

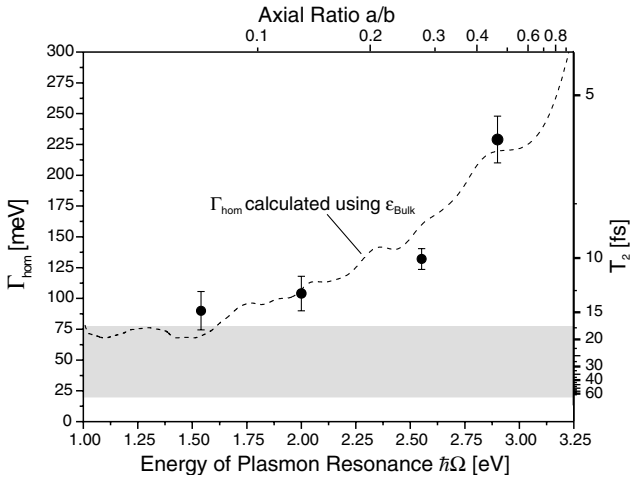

FIG. 3. Homogeneous linewidth and dephasing time of SP excitation in silver NPs on sapphire substrates as a function of the energy of the SP resonance. For further details, see text.

damping with increasing SP energy leading to a decrease of T_2 from 14.7 to 5.8 fs as the energy is raised from 1.54 to 2.9 eV. For comparison, Γ_{hom} and T_2 as deduced from Drude-relaxation times [17] are given in Fig. 3 as the gray area, revealing a remarkable difference to the experimental and calculated values for SP energies above 1.5 eV. We ascribe the observed increase of damping to the growing overlap of the SP resonance with the interband transitions of silver as the SP resonance shifts to higher energies. Since in the investigated size regime the resonance position of the SP is determined mainly by the NP shape, Fig. 3 reflects the dependence of T_2 on the axial ratio, that can be determined using electrodynamics theory [1] (upper axis). As a consequence, a precise control of the NP shape is necessary in order to determine T_2 as a function of NP size.

In the remaining part of this Letter, the influence of NP size and the chemical surrounding on T_2 will be discussed. For the influence of the reduced NP dimension on the dephasing time, classical as well as quantum-mechanical models predict a $1/r$ dependence for the inverse dephasing time [1,18–22]

$$\frac{1}{T_2(r)} = \frac{1}{T_{2,\infty}} + \frac{\hat{A}}{r}\,, \tag{3}$$

where the parameter $\hat{A}$ quantifies the influence of the NP surface on the dephasing process. Classically, the phase coherence of the collective oscillation is disturbed because of additional collisions of the electrons with the surface [22]. The loss of coherence can be further accelerated if adsorbates are present on the surface, since the conduction electrons can tunnel into and out of adsorbate states. Because of the statistic nature of the tunneling process, coherence is lost, i.e., the adsorbate leads to additional dephasing, a mechanism called *chemical interface damping* (CID) [21,22].

Since clusters with a fixed mean axial ratio are needed in order to investigate T_2 as a function of NP size, samples for such experiments were prepared with a novel method, enabling us to control the NP shape independently of size [23]. Employing this technique, silver NPs were made on sapphire and quartz surfaces under simultaneous irradiation with ns–laser pulses of a photon energy of 2.33 eV and a fluence of 160 mJ/cm^2. As a result, the SP resonances of the NPs were fixed at a photon energy of $\hbar\Omega \approx 3.0$ eV, i.e., the axial ratio remained constant. As the second step, spectral hole burning with a photon energy of 2.9 eV was applied to these NPs of different equivalent radius in order to determine the homogeneous linewidth of the SP. The results are summarized in Fig. 4. The gray lines mark a dephasing time of 6 fs that is evaluated with Eq. (2) using the dielectric function of Ref. [16]. For silver NPs on sapphire, T_2 is independent of NP size for 3.5 nm $\leq r \leq$ 10 nm, Fig. 4(a) (•). The values in this size regime are identical to the calculated value of 6 fs within their error bars of typically 1 fs. A further reduction of the NP radius to 2 nm leads to a decrease of T_2 to values as low as 4.2 fs. A least square fit of expression (3) to the experimental data gives an $\hat{A}$ factor of 0.16 nm/fs and a limiting value for large particles of $T_{2,\infty} = 7$ fs, Fig. 4(a) (dashed line). For silver NPs on quartz surfaces, on the other hand, the measured values of T_2 differ by 1 fs from the calculated value already for particles as large as $r = 10$ nm, Fig. 4(b) (•).

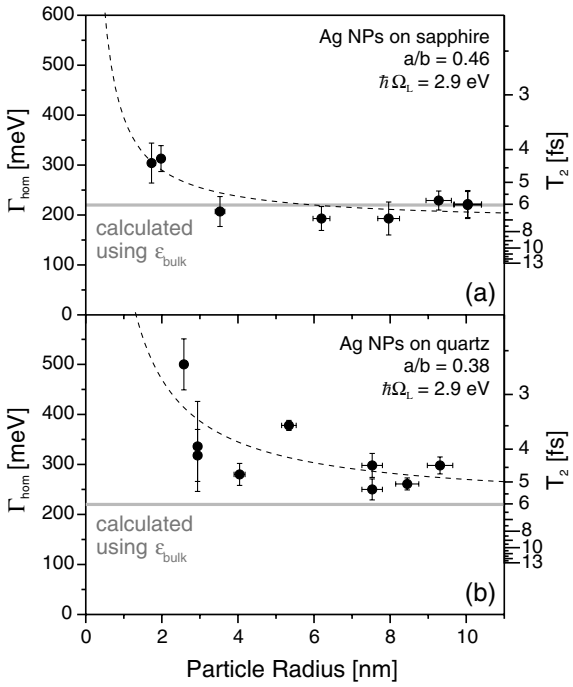

FIG. 4. Homogeneous linewidth and dephasing time of SPs in silver NPs as a function of NP size. For details, see text.

The decrease of T_2 with diminishing r is much steeper for this nanoparticle-substrate combination, leading to dephasing times as small as 2.6 fs. The $\hat{A}$ parameter is determined in this case to be 0.38 nm/fs, and the limiting value is $T_{2,\infty} = 6$ fs, Fig. 4(b) (dashed line).

Whereas the limiting value of T_2 is the same for both substrates within the experimental error, the $\hat{A}$ parameters differ by a factor of 2.4. Possible reasons for that are differences in (i) the efficiency of CID due to different substrate materials, and therefore different surface-adsorbate states, and (ii) the size of the contact area between the NP and the substrate. In order to estimate the fraction of the contact area between the NP and the substrate of the entire NP surface, the Yamaguchi theory [24], which allows for the calculation of a nominal contact area, was applied [14]. As a result, a fraction of 32% for both substrate materials was calculated. Consequently, the difference of the $\hat{A}$ parameters by a factor of 2.4 has to be ascribed to different CID efficiency. To our knowledge the only quantitative theory that describes the influence of the chemical environment is the treatment of Persson [21]. While for a free silver NP, Persson computed an $\hat{A}$ parameter of $\hat{A}_{\mathrm{Vak}} = 0.2$ nm/fs, a value of $\hat{A}_{\mathrm{SiO_2}} = 0.75$ nm/fs for a silver cluster embedded in a SiO_2 matrix was obtained. For Al_2O_3, no calculations are available yet. In order to compare our experimentally determined $\hat{A}$ parameters for silver NPs on quartz with the Persson model, the $\hat{A}$ parameters of the theory have to be weighted with the fraction of the contact area between NP and substrate. Taking into account a value of 32 % as discussed above, the theoretical value for our supported NPs is $\hat{A} = 0.38$ nm/fs. This value is exactly the $\hat{A}$ parameter experimentally determined here. Our $\hat{A}$ factor for silver NPs on sapphire on the other hand compares best to the value $\hat{A}_{\mathrm{Vak}}$ for free NPs in the Persson model. We therefore conclude that quartz as a substrate material substantially contributes to CID. In turn, we do not observe CID for silver NPs on sapphire surfaces. A possible reason for this difference is the separation between the conduction band of the oxide and the Fermi level of the NPs, which amounts to 2.6 eV for quartz [21]. This makes possible direct injection of electrons from the conduction band of the NP into the conduction band of the substrate, which is known to be an important damping mechanism for titanium oxide surfaces [13]. In contrast, an energy of at least 3.8 eV is needed for the process on sapphire substrates, which surmounts the SP energy by nearly 1 eV [25]. Nevertheless, as far as Ag NPs on sapphire are concerned, a rigorous theoretical treatment of CID is highly desirable.

In summary, the combination of laser assisted NP growth with persistent spectral hole burning makes possible systematic investigation of the dephasing of SPs in metal NPs. A striking dependence of T_2 in silver NPs on the SP energy was revealed, reflecting the influence of the bulk properties of the cluster material on the ultrafast dephasing, thus reducing T_2 with increasing axial ratio of the NPs. Most importantly, for silver NPs on sapphire, the reduced dimension influences T_2 for radii below 4 nm in agreement with theoretical predictions for pure surface scattering [21]. On quartz substrates, the size dependence is much more pronounced and, consequently, the NP dimensions determine T_2 already at NP sizes of $r = 10$ nm. The strong damping observed on quartz surfaces is ascribed to CID and agrees well with theoretical predictions [21].

Financial support by the *Deutsche Forschungsgemeinschaft* and the *Fonds der Chemischen Industrie* is gratefully acknowledged. We thank Professor A. Goldmann for providing the BBO-OPO. T.V. is grateful also to the DAAD and the RFBR (Grant No. 00-02-16865).

*Electronic address: j.bosbach@physik.uni-kassel.de
†Permanent address: Vavilov State Optical Institute, P.O. Box 953, St. Petersburg 197101, Russia.

[1] U. Kreibig and M. Vollmer, *Optical Properties of Metal Clusters* (Springer, Berlin, 1995).
[2] F. Stietz *et al.*, Phys. Rev. Lett. **84**, 5644 (2000).
[3] T. Vartanyan *et al.*, Appl. Phys. B **73**, 291 (2001).
[4] C. Sönnichsen *et al.*, Phys. Rev. Lett. **88**, 077402 (2002).
[5] T. Klar *et al.*, Phys. Rev. Lett. **80**, 4249 (1998).
[6] B. Lamprecht *et al.*, Appl. Phys. B **69**, 223 (1999).
[7] Y.-H. Liau *et al.*, J. Phys. Chem. B **105**, 2135 (2001).
[8] S. Nie *et al.*, Science **275**, 1102 (1997).
[9] K. Sokolov *et al.*, Anal. Chem. **70**, 3898 (1998).
[10] L. Novotny *et al.*, Phys. Rev. Lett. **79**, 645 (1997).
[11] R. F. Haglund, Jr., *et al.*, Opt. Lett. **18**, 373 (1993).
[12] T. Vartanyan *et al.*, Appl. Phys. B **68**, 425 (1999).
[13] N. Nilius *et al.*, Chem. Phys. Lett. **349**, 351 (2001).
[14] T. Wenzel *et al.*, Surf. Sci. **432**, 257 (1999).
[15] A. Wokaun *et al.*, Phys. Rev. Lett. **48**, 957 (1982).
[16] D. Edward and I. Palik, *Handbook of Optical Constants of Solids* (Academic Press, Orlando, Florida, 1985).
[17] C. L. Foiles, in *Numerical Data and Functional Relationships in Science and Technology*, edited by K.-H. Hellwege and J. L. Olsen, Landolt-Börnstein, New Series, Group III, Vol. 15, Part b (Springer, Heidelberg, 1985), p. 213.
[18] F. Calvayrac *et al.*, Phys. Rep. **337**, 493 (2000).
[19] C. Yannouleas *et al.*, Ann. Phys. (N.Y.) **217**, 105 (1992).
[20] A. Kawabata *et al.*, J. Phys. Soc. Jpn. **21**, 1765 (1966).
[21] B. Persson, Surf. Sci. **281**, 153 (1993).
[22] U. Kreibig *et al.*, Ber. Bunsen-Ges. Phys. Chem. **101**, 1593 (1997).
[23] T. Wenzel *et al.*, Appl. Phys. B **69**, 513 (1999).
[24] T. Yamaguchi *et al.*, Thin Solid Films **21**, 173 (1974).
[25] S. Ciraci *et al.*, Phys. Rev. B **28**, 982 (1983).